Simulating Time Dependent Diffusive Shock Acceleration in the Transition Region

S. Aerdker,[a,b,*] **L. Merten,**[a,b] **J. Becker Tjus,**[a,b,c] **D. Walter,**[a,b] **F. Effenberger**[a,b] **and H. Fichtner**[a,b]

[a]*Theoretical Physics IV, Plasma Astroparticle Physics, Faculty for Physics and Astronomy, Ruhr University Bochum, 44780 Bochum, Germany*

[b]*Ruhr Astroparticle and Plasma Physics Center (RAPP Center), Germany*

[c]*Department of Space, Earth and Environment, Chalmers University of Technology, 412 96 Gothenburg, Sweden*

E-mail: sophie.aerdker@rub.de, lukas.merten@rub.de, julia.tjus@rub.de, dw@tp4.rub.de, fe@tp4.rub.de, hf@tp4.rub.de

The origin of high-energy cosmic rays (CRs) in the transition region between the knee and the ankle is still debated. In general, CRs are most likely accelerated stochastically in time-dependent, turbulent magnetic field structures. Diffusive Shock Acceleration at stationary shocks produce the characteristic power-law spectrum with the spectral slope depending only on the shock's compression ratio. The spectrum that is observed downstream can be modulated by properties of diffusive transport. Typical questions are: How do a finite shock width and diffusion properties influence the time evolution of the spectrum? And, how does it change when cosmic rays are already pre-accelerated to a power-law spectrum when they enter the acceleration region?

We assess those questions using the stochastic differential equation solver (DiffusionSDE) of the cosmic-ray propagation framework CRPropa3.2. Assuming continuous injection of CRs in the acceleration region, the time evolution of the spectrum at a spherical shock is obtained for energy-independent and energy-dependent diffusion. We show that the energy spectrum at the shock may be steeper than the ideal shock spectrum. The injection of pre-accelerated cosmic rays can lead to a broken power-law spectrum.

We apply our findings to the re-acceleration of cosmic rays at the Galactic Wind Termination Shock (GWTS). First results of modelling a spherically symmetric GWTS and a spiral Galactic magnetic field are presented. We conclude that time-resolved simulations are necessary to constrain the contribution of GWTS to the CR flux, considering a finite shock lifetime, finite shock width, energy-dependent diffusion, complex magnetic field, and upstream cooling.

*Speaker

1. Introduction

The origin of high-energy cosmic rays (CRs) between the spectral "knee" and "ankle" is still debated. It is believed, that the transition from Galactic to extra-galactic origin occurs in the energy range from $\sim 10^{15}\,\text{eV} - 10^{18}\,\text{eV}$ [4]. CRs are most likely accelerated stochastically, e.g. by Diffusive Shock Acceleration (DSA). CRs are scattered on both sides of a shock and may cross the shock front repeatedly. Each time they cross the shock, they are accelerated depending on their energy.

The Galactic Wind Termination Shock (GWTS) that may form when the supersonic Galactic wind slows down due to interaction with the Intergalactic Medium (IGM) might contribute to the sources of CRs [11, 13]. CRs originating in the Galactic disk are advected outwards and are re-accelerated to higher energies at the GWTS. A fraction of high-energy CRs may be able to propagate back to the Galaxy against the Galactic wind. Particle acceleration at the GWTS was already discussed e.g. by [7], [13], [11], and recently by [12].

In order to estimate the contribution of the GWTS to the CR spectrum, not only the propagation from the GWTS back to the Galaxy is of importance but also the acceleration process itself. Based on our recent analysis of time-dependent DSA considering various shock and magnetic field configurations [2], we investigate the impact of a finite shock width, energy-dependent diffusion, a radial wind profile, and a spiral magnetic field on the energy-spectrum at the shock. We also discuss the effect on the probability of CR to escape upstream and propagate back to the Galaxy.

2. Modeling Diffusive Shock Acceleration with CRPropa3.2

In this section we briefly introduce CRPropa3.2 [3] as a framework for simulating DSA, focusing on spherical shocks. For a detailed study on modeling DSA with CRPropa3.2 we refer to [2].

In the diffusive regime, CR transport can be described by the Fokker-Planck equation

$$\frac{\partial n}{\partial t} + \vec{u} \cdot \nabla n = \nabla \cdot (\hat{\kappa} \nabla n) + \frac{1}{p^2}\frac{\partial}{\partial p}\left(p^2 D \frac{\partial n}{\partial p}\right) + \frac{1}{3}\left(\nabla \cdot \vec{u}\right)\frac{\partial n}{\partial \ln p} + S(\vec{x}, p, t) \quad . \tag{1}$$

The time evolution of the CR number density n in space $\vec{x}$ and momentum $p = |\vec{p}|$ is given by the advection with a background flow $\vec{u}$, spatial diffusion described by the diffusion tensor $\hat{\kappa}$, momentum diffusion described by the coefficient D, adiabatic energy changes and CR sources S.

For simulating DSA with CRPropa3.2 the `DiffusionSDE` module is used [10]. Instead of integrating the partial differential equation (1) the corresponding set of Stochastic Differential Equations (SDEs) is integrated using the Euler-Maruyama scheme. Neglecting momentum diffusion in eq. (1) and considering only energy-dependent diffusion, the Fokker-Planck type equation can be transformed into

$$\mathrm{d}\vec{x} = \vec{u}(x)\,\mathrm{d}t + \sqrt{2\hat{\kappa}}\,\mathrm{d}\vec{\omega}_t, \quad \mathrm{d}p = -\frac{p}{3}\nabla \cdot \vec{u}\,\mathrm{d}t, \tag{2}$$

where $\mathrm{d}\vec{\omega}_t = \sqrt{\mathrm{d}t}\,\vec{\eta}$ is a Wiener process with Gaussian distributed random numbers η_i. Equation (2) describes the time evolution of a phase-space element — also called pseudo-particle — instead

of real physical trajectories. The momentum equation is an ordinary differential equation. Pseudo-particles are propagated along and perpendicular to the magnetic field. The diffusion tensor

$$\hat{\kappa} = \kappa_{\parallel} \begin{pmatrix} \epsilon & 0 & 0 \\ 0 & \epsilon & 0 \\ 0 & 0 & 1 \end{pmatrix} \left(\frac{E}{E_0} \right)^{\alpha}, \tag{3}$$

is defined in local magnetic field coordinates, is constant in space and may depend on energy. For large curvature radii of the magnetic field lines, the diffusion coefficients for the normal and binormal direction of the magnetic background field line can be assumed to be the same.

2.1 Simulation Set-Up and Analysis

The simulation is set-up with the `DiffusionSDE` module which handles the spatial displacement by taking into account the magnetic field lines from the `MagneticField` module. In the following the magnetic field is assumed to be radial or an Archimedean spiral. In the diffusive picture, acceleration at the shock comes from the adiabatic heating term in eq. (2), which is modeled by the `AdiabaticCooling` module, that depends on the `AdvectionField`, here given by [11]:

$$\vec{u}(r) = u_1 \left\{ 1 + \left[\left(\frac{R_{\text{sh}}}{2r} \right)^2 \frac{1}{1 + e^{-\frac{r - R_{\text{sh}}}{L_{\text{sh}}}}} \right] \right\} \vec{e}_{\text{r}} \quad . \tag{4}$$

The upstream wind speed u_1 is constant, downstream it decays with r^{-2}, thus, particles are not subject to adiabatic cooling. The shock width is given by the parameter L_{sh}. A strong shock with a compression ratio of $q = 4$ is considered.

Pseudo-particles with energy E_0 are injected at $t = 0$ at the shock $r = R_{\text{sh}}$ and simulated until a specified time T. Current energy and position of the pseudo-particles are stored during simulation. In the later analysis, the energy spectrum $J(E) = dN/dE$ of particles at time T_i is approximated by the histogram $\Delta N/\Delta E$, ΔN is the number of pseudo-particles in each energy bin ΔE. Energy is binned with equal distance in logarithmic space and the error for each bin is then given by $\Delta J = J/\sqrt{\Delta N}$. The statistics at high energies can be enhanced by adding the `CandidateSplitting` module. During simulation candidates are split in copies once they cross specified energy boundaries and are weighted accordingly in the later analysis (see [2] for more details).

In order to obtain the energy spectrum at the shock, the analysis is restricted to pseudo-particles close to the shock, e.g. $r = [r_{\text{sh}}, r_{\text{sh}} + r_{\text{bin}}]$ for a spherical shock of radius r_{sh} and bin width r_{bin}. Considering the GWTS, we expect a stationary flux of particles to arrive at the shock, which can be approximated with the `TimeEvolutionObserver` (see [2, 10] for details).

In order to obtain the correct spectra, pseudo-particles need to encounter the changing advection field when propagating across the shock. The probability to hit the shock increases with decreasing time step or increasing shock width when the advection speed and diffusion are fixed. However, increasing the shock width may change the resulting spectrum as discussed in Section 3.1. In order to numerically reproduce the ideal shock spectrum [8] proposed that the inequality

$$u \Delta t < L_{\text{sh}} \lesssim \sqrt{\kappa \Delta t} \tag{5}$$

3

must be fulfilled, so that the advective step is smaller than the shock width and the diffusive step greater than the shock width. The latter ensures that diffusion is strong enough for particles to go back over the shock. Thus, the inequality combines numerical and physical constraints for the simulation of DSA with SDEs.

3. Modeling DSA at the GWTS

3.1 Spectrum at a spherical GWTS

Considering an ideal shock, the energy spectrum at the shock only depends on the shock's compression ratio with the spectral slope $s = 2 - 3q/(q - 1)$ (e.g. [6]). However, this does not necessarily apply to shocks with a finite width. Depending on the ratio of advection speed, diffusion strength, and shock width the spectrum may be steeper indicating less efficient acceleration. Analytical approximations for the resulting spectral slope were done for one-dimensional planar shocks and energy-independent diffusion by [8] and [1].

We consider a spherical GWTS with similar parameters as in [11]: shock width $L_{sh} = 50\,pc$, diffusion coefficient $\kappa = 5 \cdot 10^{24}\,m^2/s$, and upstream advection speed of $u_1 = 600\,km/s$ with a compression ratio $q = 4$. Here, diffusion is assumed to be parallel to the shock normal, thus it is scaled down compared to the work of [11] where an Archimedean spiral magnetic field is considered as in Section 3.3. According to [1] the ratio $u_1 L_{sh}/\kappa \approx 0.185$ leads to a slightly steeper spectrum $s \approx 2.2$.

Figure 1 compares the time evolution of the energy spectrum at a spherical shock with diffusion κ parallel to the shock normal for different values of the shock width and diffusion coefficient by keeping $u_1 = 600\,km/s$. The spectra are weighted with E^2 to highlight deviations from the slope $s = -2$ of an ideal shock. The middle plot shows the GWTS configuration similar to [11]. Clearly, the energy spectrum is steeper with $s < -2$. With smaller shock width (left), the ideal shock spectrum is recovered. Also, stronger diffusion (right) leads to the ideal shock spectrum. However, acceleration at the shock is slower due to higher diffusion. Thus, with the shock being active for 80 Myr, the maximal energy is only 1/5 of the energy that may be reached with $L_{sh} = 5\,pc$ and $\kappa = 5 \cdot 10^{24}\,m^2/s$.

CRs reaching the GWTS are already pre-accelerated up to a maximal energy E_{max} that can be reached by accelerators in the Galaxy. Depending on the shock and diffusion properties they likely have a spectrum of $s = -2$. With the spectrum at the GWTS being steeper, the injected spectrum would predominate for energies $E < E_{max}$. Above that energy, $E > E_{max}$, particles are re-accelerated to the shock spectrum, which may lead to a slight break in the spectrum.

Figure 2 shows the time evolution at the shock when a pre-accelerated spectrum with slope -2 from $E = [10^{12}, 10^{15}]\,eV$ is injected. With the diffusion coefficient $\kappa = 5 \cdot 10^{24}\,m^2/s$ particles are re-accelerated to higher energies with a steeper spectrum. With the diffusion coefficient $\kappa = 50 \cdot 10^{24}\,m^2/s$ particles are re-accelerated to the ideal shock spectrum, however, the acceleration time scale is longer.

3.2 Energy-dependent diffusion

Taking energy-dependence into account, the diffusion coefficient increases with energy, thus, with the life time of the shock. Higher diffusion leads to flatter spectra up to the limit given by
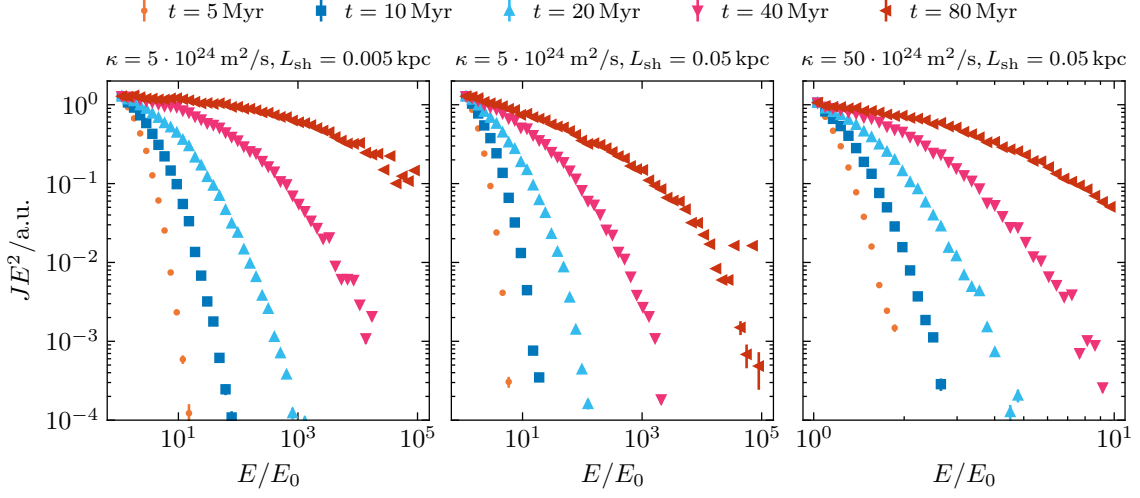
Figure 1: Time evolution of the energy spectrum at a spherical shock with width L_{sh} and diffusion κ parallel to the shock normal. The upstream advection speed is $u_1 = 600\,\mathrm{km/s}$ and the compression ratio is $q = 4$.
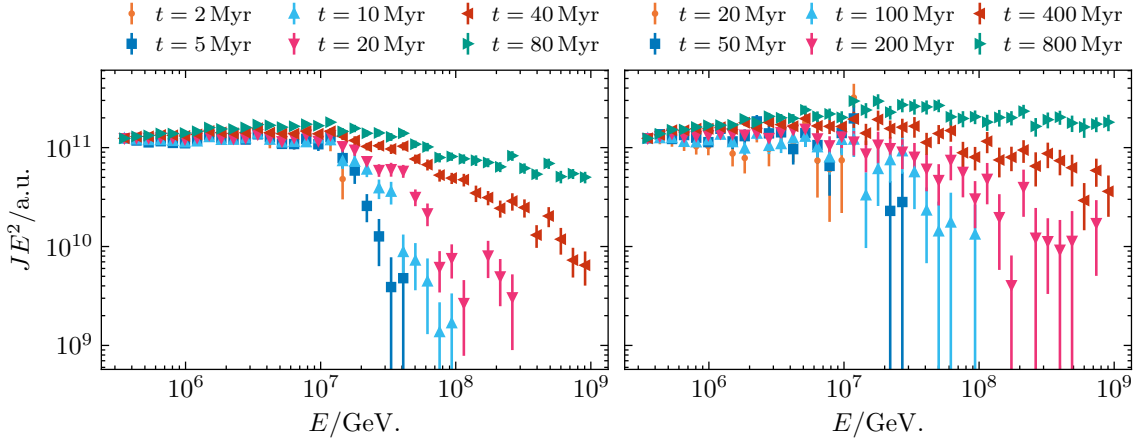

Figure 2: Time evolution of the re-acceleration of particles at a spherical shock. Pre-accelerated spectra with $E_{\max} = 10^{15}\,\mathrm{eV}$ and slope $s = -2$ is injected at the shock. $u_1 = 600\,\mathrm{km/s}$, $L_{\mathrm{sh}} = 50\,\mathrm{pc}$. Left: Diffusion coefficient $\kappa = 5 \cdot 10^{24}\,\mathrm{m^2/s}$. Particles are re-accelerated to a steeper spectrum. Right: $\kappa = 50 \cdot 10^{24}\,\mathrm{m^2/s}$. Particles are re-accelerated to the -2-spectrum.

an ideal shock with compression of $q = 4$, but also slows down the acceleration process. Figure 3 shows the energy spectrum at the shock and number density in the acceleration region for a shock width $L_{\mathrm{sh}} = 0.05\,\mathrm{kpc}$ and $\kappa(E) = 5 \cdot 10^{24}\,\mathrm{m^2/s}\,(E/E_0)^{0.6}$ compared to energy-independent diffusion. The energy-dependent diffusion coefficient is normalized with $E_0 = 10^{15}\,\mathrm{eV}$.

For energy-dependent diffusion, with increasing energy, diffusion is higher than for the energy-independent case. Thus, the energy spectrum of a strong shock is reproduced. With increasing diffusion, acceleration is slowed down. For energy-dependent diffusion, at $t = 400\,\mathrm{Myr}$ the spectrum still evolves and the energy cut-off at $\approx 10^8\,\mathrm{GeV}$ is visible. For energy-independent diffusion, at $t = 100\,\mathrm{Myr}$ the stationary solution for $E < 10^9\,\mathrm{GeV}$ is already reached.

The most interesting difference in the number density is in the upstream region. Considering energy-dependent diffusion, over time particles are more likely to reach the far upstream region due to higher diffusion. The upstream energy-spectrum differs from the spectrum at the shock, since only high energy particles are able to contribute. Thus, particles escaping the acceleration region upstream and propagate back to the Galaxy, likely were accelerated to the highest energies.
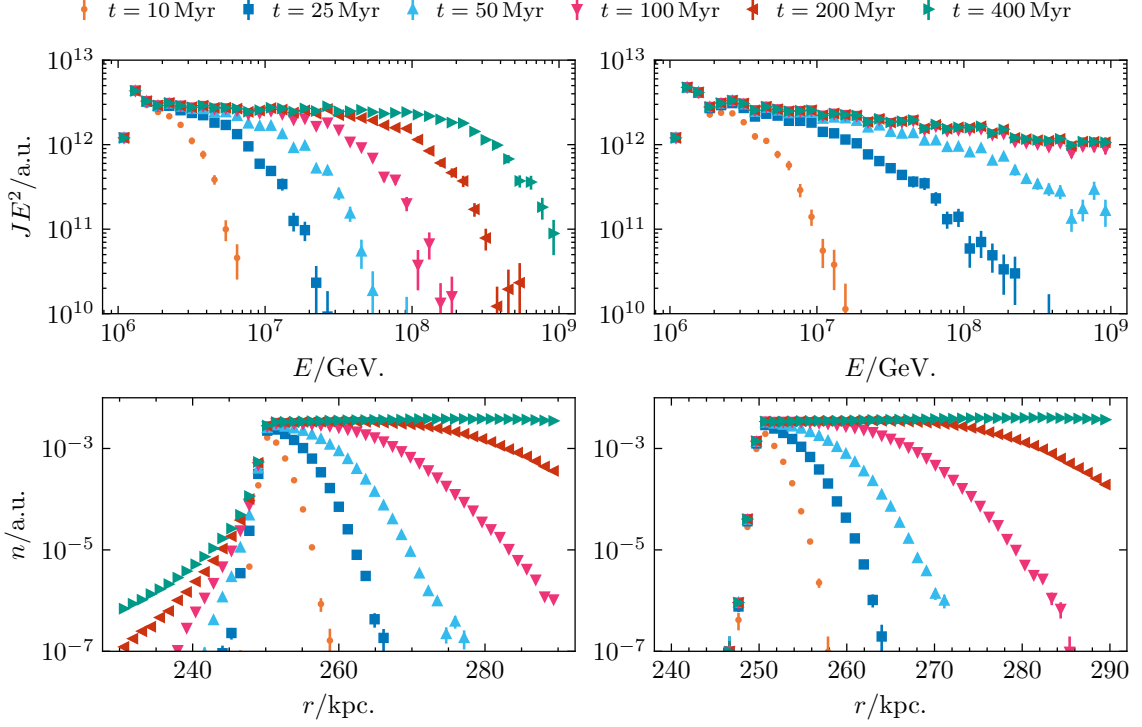

Figure 3: Time evolution of the spectrum at the shock (top) and number density close to the shock (bottom) with energy dependent diffusion, $\kappa(E) = 5 \cdot 10^{24}\,\mathrm{m}^2/\mathrm{s}\,(E/E_0)^{0.6}$ (left) and energy independent diffusion (right), $\kappa(E) = 5 \cdot 10^{24}\,\mathrm{m}^2/\mathrm{s}$.

Particles in the upstream region experience adiabatic cooling due to the expanding wind. Thus, the acceleration time scale is longer and the maximal energy that can be reached at the shock is lower compared to planar shocks.

3.3 Spiral Magnetic Field

We consider an Archimedean spiral magnetic field that better resembles the Galactic magnetic field than the radial field from the previous simulations. Having a spherical shock, this leads to a perpendicular shock in the Galactic disk, where magnetic field lines are almost perpendicular to the shock normal, and parallel shock at the poles, $\theta = 0$. In between the shock can be considered oblique.

Acceleration is influenced by the effective diffusion across the shock. Depending on the ratio of parallel to perpendicular diffusion, the effective diffusion changes with latitude. This leads to differences in the acceleration time, but also in the spectrum produced by the shock when effective diffusion length becomes short compared to the assumed shock width. In the Galactic disk, the

shock is perpendicular. If only parallel diffusion is considered, there is no acceleration at all, since particles are not able to cross the shock. Effective diffusion is, thus, lowered from the poles to the equator. This again, may lead to broken-power law spectra if the pre-accelerated energy spectrum is harder than the one produced by the shock. To which spectral slope it breaks at the shock then depends on latitude. A similar dependency was already found by [5] for SNRs.
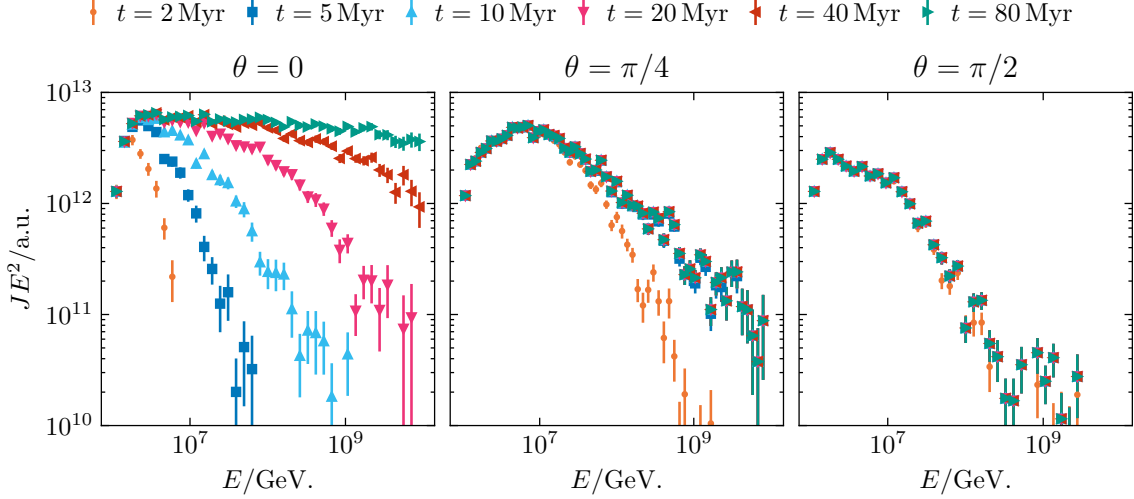

Figure 4: Time evolution of the energy spectrum at a spherical GWTS. With a spiral magnetic field, effective diffusion parallel to the shock normal varies with latitude. Left: $\Theta = [0, \pi/10]$. At the poles effective diffusion is highest, leading to the flattest spectrum but also long acceleration times. Middle: $\Theta = [\pi/4 - \pi/20, \pi/4 + \pi/20]$, oblique shock. Right: $\Theta = [\pi/2 - \pi/20, \pi/2 + \pi/20]$, shock is almost perpendicular, time evolution is fast but spectrum is steeper.

Taking anisotropic diffusion into account, acceleration is also possible in the Galactic disk and the difference in acceleration time scale and energy spectrum are less drastic. Also perpendicular diffusion impacts the arrival times and anisotropy of the spectrum observed at Earth [11].

4. Discussion

The spectrum at a potential GWTS is influenced by the ratio of the wind speed, shock width and effective diffusion parallel to the shock normal. Considering a wide GWTS, e.g. due to nonlinear interaction between the shock and CRs [9], the produced energy-spectrum may be steeper than the pre-accelerated spectrum of CRs arriving at the GWTS. This may lead to broken-power law spectra.

The ratio of the shock width to effective diffusion length may also be impacted by the magnetic field. Considering a spiral magnetic field, the spectral slope of the energy spectrum at the shock may change with latitude. The result could be a break in the energy spectrum which increases from pole to the Galactic disk. How this may impact the observed spectrum at Earth has to be studied in future simulations also taking the propagation back to the Galaxy into account. Likely the difference is smoothed out due to diffusion. However, the difference in the length of magnetic field lines impacts the arrival time of particles [11]. Since the field lines at the poles are shorter than the ones in the Galactic plane, a shift in the maximal energy and break of the spectrum over time could be visible in simulations.

The maximal energy that can be reached at a spherical shock depends on the wind speed, shock radius and diffusion strength. Introducing energy-dependent diffusion, acceleration at the shock is slowed down over time with increasing diffusion. Considering a finite lifetime of the GWTS, depending on the acceleration time scale, the maximal energy might not be reached within its lifespan. With energy-dependent diffusion, high-energy CRs are more likely to escape upstream. Taking a finite shock lifetime into account, the probability to propagate back to the Galaxy increases when the wind slows down over time.

CRs that are advected out of the Galaxy are subject to adiabatic cooling, which lowers the maximal energy of the pre-accelerated spectrum. CRs that are re-accelerated at the GWTS and escape upstream also experience cooling. For the GWTS to contribute to the CR spectrum in the transition region, energy gain due to acceleration must exceed the energy loss due to cooling.

We conclude that a study, taking into account the propagation of pre-accelerated CRs out of the Galaxy, re-acceleration at the GWTS and propagation back is necessary to assess the contribution of the GWTS to the transition region. Upstream cooling and a finite shock lifetime, thus, a time-dependent radial wind profile should be considered. Diffusion along a realistic magnetic field should be energy-dependent and anisotropic.

Acknowledgments

References

[1] A. Achterberg & K. M. Schure, MNRAS 411 (2011) 2628 [arXiv:1103.3049]

[2] S. Aerdker et al., arXiv e-prints (2023) [arXiv.2306.10802]

[3] R. Alves Batista et al., JCAP 2022 (2022) 035 [arXiv:2208.00107]

[4] J. Becker Tjus & L. Merten, Phys. Rep. 872 (2020) 1 [arXiv:2002.00964]

[5] P. L. Biermann et al., Phys. Rev. Letters, 2009 [doi:10.48550/arXiv.0903.4048]

[6] L. O. Drury, Rep. Prog. Phys 46 (1983) 973

[7] J. R. Jokipii & G. Morfill, ApJ 312 (1987) 170

[8] W. M. Krülls & A.Achterberg, A&A 286 (1994) 314

[9] J. A. le Roux et al., J. Geophys. Res. 101 (1996) 4791.

[10] L. Merten et al., JCAP 2017 (2017) 046 [arXiv:1704.07484]

[11] L. Merten et al., ApJ 859 (2018) 63 [arXiv:1803.08376]

[12] P. Mukhopadhyay et al, arXiv e-prints (2023) [arXiv:2301.08902]

[13] S. Thoudam et al, A&A 595 (2016) A33 [arXiv:1605.03111]